Pulse Shaping in Non-Coherent DLL Tracking of CDMA Signals

Mohamed Adnan Landolsi and Ganiyu B. Hussain
Electrical Engineering Department
King Fahd University of Petroleum & Minerals
P.O. Box 1413, Dhahran 31261
Saudi Arabia
{andalusi,ghussain}@kfupm.edu.sa

Abstract: - The paper analyses the impact of pulse shaping on code tracking for direct-sequence code division multiple access (DS-CDMA) signal synchronization using non-coherent delay-lock loops (NC-DLL). The dependency of the residual timing error variance on the chip waveform is emphasized, and the performance of several non-rectangular pulse shapes is presented. The design of optimized chip waveforms for minimizing the DLL tracking error variance is then formulated using a cost function expressed in frequency-domain and highlighting the dependency of the tracking jitter on the chip waveform Fourier transform. A solution methodology is introduced based on the use of Prolate Spheroidal Wave Functions. Some illustrative design examples are presented, establishing theoretical limits for the best achievable performance (minimum jitter). In particular, it is shown that the half-sine and Hamming pulses are near-optimum when considering pulses with 99% and 99.9% in-band power bandwidth occupancies, respectively.

Key-Words: - CDMA, DLL, Code tracking, Tracking jitter, Chip waveform shape.

1 Introduction

For DS-CDMA systems, chip timing alignment between the received and the locally generated signature sequences (or spreading codes) must be achieved prior to data demodulation. Code timing synchronization is typically achieved in two steps: code acquisition and code tracking [1,2]. First, during acquisition, the receiver obtains the relative delay between the received and the locally generated codes to within a chip interval. Then, in the subsequent tracking phase, finer timing adjustment is performed in order to bring the residual timing error as close to zero as possible.

In this paper, we focus on code tracking which is typically implemented by means of the classical early-late delay-locked loop (DLL) that has been thoroughly discussed in the spread spectrum literature (see [1] and references therein). Linear and nonlinear DLL models have been presented, and the tracking error jitter and mean-time-to-lose are derived as key performance indicators. In our case, we adopt the linear DLL model (applicable for practical SNR ranges), for which the DLL performance is essentially determined by the characteristics of the discriminator S-curve [1,2], which depend on the correlation properties of the early-late spread-spectrum waveforms.

Quite importantly, in addition to the correlation properties of the spreading codes, it is also found that another important factor that affects several performance aspects of DS-CDMA systems is the actual shape of the chip waveform pulse. The impact of chip waveform shaping has been addressed from the perspective of multiple-access interference and error performance analysis (e.g., [3,4,5]). There have also been some limited studies of this impact on code synchronization. For example, in [6], acquisition and tracking aspects of different chip waveforms are compared, and other similar comparisons appear in [7,8]. In [9], it is shown that the use of unmatched chip pulses can reduce tracking error variance. Most of these works have mainly focused on comparing different "conventional" pulse shapes, and did not undertake any optimization of the chip waveforms in order to maximize performance. Recently, in [11], such optimization is discussed in the context of timing acquisition. On the other hand, for code tracking, a coherent DLL is considered in [10], and some optimized chip waveforms are presented. However, in practice, the non-coherent DLL (NC-DLL) architecture is preferable because of its insensitivity to data modulation and carrier phase synchronization.

In this paper, we extend the work in [10] to NC-DLL code tracking systems. First, we present a comprehensive performance analysis and comparison of the impact of several common (non-rectangular) chip waveforms on code tracking jitter. In a second part, a constrained optimization problem for minimizing the residual error variance is defined and solved using Prolate Spheroidal Wave Functions [12].

The rest of the paper is organized as follows. In Section 2, the system model is presented. In Section 3, the performance analysis of the NC-DLL is discussed using a frequency domain formulation and comparative results for some conventional chip pulses are presented. In Section 4, the optimized pulse shaping procedure is discussed, and several design examples are then given in Section 5, followed by final conclusions in Section 6.

2 System Model

We consider a general CDMA system model where the signal from a given intended user is received after some transmission delay, and is given by:

$$r(t) = \sqrt{2P}\,c(t-\tau_o)\cos(\omega_o t + \phi) + n_{\mathrm{MAI}}(t) + n_{\mathrm{th}}(t) \quad (1)$$

where P is the signal power, τ_o is the propagation delay, ϕ is the carrier phase (that includes the time delay effect), $n_{th}(t)$ is the additive white gaussian noise with two-sided power spectral density $N_o/2$, and $n_{th}(t)$ is the multiple-access interference term which can also be modeled as additive gaussian noise (by invoking the central limit theorem, for a large number of co-users). The spread-spectrum waveform $c(t)$ is assumed to use a long random PN code, and is given by:

$$c(t) = \sum_{n=-\infty}^{\infty} c_n h(t - nT_c) \quad (2)$$

with $\{c_n\}$ representing a binary ± 1 chip sequence, and $h(t)$ the chip waveform pulse defined over the chip interval $[0, T_c]$. The model used is applicable for a pure pilot signal without data modulation since we mainly focus on code tracking using a non-coherent delay-locked loop (to be discussed next). We also note that, for simplicity, multipath fading effects are not explicitly included, but this will not impact the main theme of the paper, which is the exploration of the impact of pulse shaping on PN code tracking.

A non-coherent delay lock loop (NC-DLL) is assumed for tracking the timing epoch of the arriving signal. The NC-DLL is based on the early-late scheme where the received signal is correlated with two locally generated, delayed code replicas, the early $c(t - \hat{\tau}_0 + \Delta)$ and late $c(t - \hat{\tau}_0 - \Delta)$ local codes, where $\hat{\tau}_0$ is the timing estimate, and 2Δ is the early-late spacing typically set to T_c. The output waveforms are filtered and squared, and the difference is used to drive the voltage controlled oscillator (VCO) to adjust the local code timing.

The loop discriminator output due to the desired signal component is obtained as [2]:

$$Z_\Delta(\varepsilon) = R^2(\varepsilon - \Delta) - R^2(\varepsilon + \Delta) \quad (3)$$

where $\varepsilon = \tau_0 - \hat{\tau}_0$ is the timing error, and $R(\tau)$ is the code sequence autocorrelation function given for a correlation period of N chips by:

$$R(\tau) = \frac{1}{NT_c} \int_0^{NT_c} c(t)c(t+\tau)\,dt \quad (4)$$

In the sequel, we resort to a frequency-domain formulation that is found to simplify the analysis of the impact of pulse shaping on DLL tracking performance, as will be highlighted next. For long PN codes modeled as random sequences, the chip autocorrelation function can be expressed as [2]:

$$R(\tau) = \int_{-\infty}^{+\infty} |H(f)|^2 \cos(2\pi f \tau)\,df \quad (5)$$

The discriminator output in (3) is known as the DLL *S-curve*, and can be normalized to yield:

$$G(s) = R^2(s - \delta) - R^2(s + \delta) \quad (6)$$

where $s = \varepsilon/T_c$ and $\delta = \Delta/T_c$ denote normalized timing error and early-late spacing variables. A block diagram illustrating the operation of the NC-DLL is shown below.
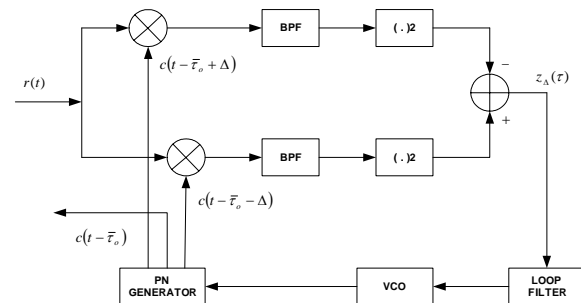
Fig. 1: Non-coherent delay-locked loop (NC-DLL).

3 Performance Analysis
3.1 DLL Tracking Error

A common performance measure of the DLL is the tracking error variance (or jitter). At high SNR, the tracking error will usually be small enough such that the loop discriminator output can be taken as a linear function of the relative timing error. Using linear loop analysis, it can be shown that an upper bound on the tracking error variance for first-order loops is approximated by [2]:

$$Var(\varepsilon) \approx \frac{2V_0^2}{N^2 E_c^2 \kappa^2} \quad (7)$$

where N is the correlation period length (in chips),

$E_c = P/T_c$ is the energy per chip, κ is the S-curve slope at the origin $(s = 0)$. The V_0 term captures the total interference variance given by:

$$V_o = N_o + I_o \qquad (8)$$

where N_0 is the AWGN contribution and I_0 is the variance of the multiple-access interference (MAI) due to other users. Since CDMA systems are mainly interference-limited, the AWGN factor can be dropped to focus exclusively on the MAI term. With equal received power P for all users, the MAI term variance can be expressed in frequency-domain as [2]:

$$I_0 \cong P(K_u - 1)M_c \qquad (9)$$

where K_u is the number of users, P is the received power, and M_c the pulse-dependent MAI factor given by [2]:

$$M_c = \int_{-\infty}^{\infty} |H(f)|^4 \, df \qquad (10)$$

with $H(f)$ denoting the Fourier transform of the chip waveform pulse $h(t)$.

It is also desirable to express the S-curve slope κ in a tractable form that emphasizes its dependency on the chip pulse shaping filter. This is readily achieved by observing that:

$$\kappa = \left. \frac{dG(s)}{ds} \right|_{s=0} \qquad (11)$$

$$= 2\left[R'(-\delta)R(-\delta) - R'(\delta)R(\delta) \right]$$

where the auto-correlation function $R(.)$ can be substituted from (5). In typical DLL designs, the value $\delta = 0.5$ is commonly used (half-a-chip early-late branch spacing), and it follows that:

$$R(0.5) = \int_{-\infty}^{+\infty} |H(f)|^2 \cos(\pi f) \, df \qquad (12)$$

On the other hand,

$$R'(0.5) = -\int_{-\infty}^{+\infty} 2\pi f |H(f)|^2 \sin(\pi f) \, df \quad (13)$$

Substituting (12) and (13) into (11) and observing that $R(\delta)$ is even and $R'(\delta)$ is odd, we finally get:

$$\kappa = 4\left[\int_{-\infty}^{+\infty} |H(f)|^2 \cos(\pi f) df \right] \\ \times \left[\int_{-\infty}^{+\infty} 2\pi f |H(f)|^2 \sin(\pi f) df \right] \qquad (14)$$

3.2 Chip Waveform Comparisons

Going back to the expression of the tracking error variance in (7), the code tracking performance can be directly estimated by evaluating the MAI variance and the NC-DLL S-curve slope κ. More specifically, it is seen that, aside from constant factors, the performance for a given pulse shape will depend on the ratio M_c/κ, which in turn depends on the pulse spectrum $H(f)$. This will form the basis for the relative performance assessment of several pulse shaping schemes, and the subsequent optimized design of these spreading waveforms, as will be discussed in the next section.

For comparative purposes, Table 1 gives a list of commonly used pulses, starting with the unit rectangular pulse $p_{T_c}(t)$ defined over the interval $[-T_c/2, T_c/2]$. Table 2 shows the normalized tracking error factor for the different pulse shapes.

Rectangular	$p_{T_c}(t)$
Half-Sine	$\sin(\pi t/T_c) \, p_{T_c}(t)$
Triangular	$(1 - |2t/T_c - 1|) \, p_{T_c}(t)$
Raised-Cosine	$[0.5 - 0.5\cos(2\pi t/T_c)] p_{T_c}(t)$
Hamming	$[0.54 - 0.46\cos(2\pi t/T_c)] p_{T_c}(t)$

Table 1: Conventional Pulse Shapes.

Pulse Shape	M_c	κ	M_c/κ
Rectangular	0.333	2.000	0.167
Half-Sine	0.293	2.000	0.147
Triangular	0.270	1.500	0.180
Raised-Cosine	0.241	0.889	0.271
Hamming	0.264	1.357	0.194

.

Table 2: Tracking Performance Comparisons.

From the results in Table 2, it is seen that the best performance is achieved by the half-sine pulse.

However, it should be pointed out that other factors (such as bandwidth confinement) play an important role as well, and this will be further discussed subsequently.

4 Performance Optimization
4.1 Problem Formulation
The waveform-dependent term in the DLL tracking error is a function of the ratio M_c/κ as shown in the previous section. Therefore, to optimize the DLL tracking performance, it is important to design pulse shaping filters $H(f)$ that minimize this quantity. The optimization should also be subject to additional signal constraints including fixed signal energy and limited bandwidth occupancy. Earlier work on the minimization of timing jitter in the coherent delay lock loop was done in [10]. We extend the approach presented in [10] and apply it to the noncoherent delay lock tracking loop NC-DLL considered in this work.

As discussed previously, the tracking error performance is optimized by minimizing a cost functional F (given by the ratio M_c/κ) over the chip filter response $H(f)$:

$$F = \frac{\int\limits_{-\infty}^{+\infty}|H(f)|^4 df}{\left[\int\limits_{-\infty}^{+\infty}|H(f)|^2 \cos(\pi f) df\right]\left[\int\limits_{-\infty}^{+\infty}2\pi f|H(f)|^2 \sin(\pi f) df\right]}$$

(15)

The minimization of this functional is subject to additional constraints including fixed pulse energy and limited bandwidth occupancy. The fixed normalized energy constraint is expressed by:

$$\int\limits_{-\infty}^{\infty}|H(f)|^2 df = 1$$

(16)

In addition, it is also desired to improve pulse bandwidth confinement so that only a small fraction η (e.g., 1%) of energy spills over a given band $[-B,B]$. In CDMA, a bandwidth efficient chip waveform allows for the use of a higher spreading factor N for a given allocated spectrum, thereby improving overall system performance. The constraint for bandwidth confinement is:

$$\int\limits_{-B}^{B}|H(f)|^2 df = 1-\eta$$

(17)

A direct, closed-form solution to this constrained optimization problem is not tractable. Instead, we propose an approach that converts the problem to an equivalent discrete formulation with reduced complexity. This is achieved by expanding the chip pulse Fourier transform $H(f)$ using an adequate set of basis functions, and then solving for the expansion coefficients that minimize the objective function F, subject to the specified constraints. Special functions known as Prolate Spheroidal Wave Functions (PSWF) [12] are particularly well suited for this and have been successfully used for similar optimization problems [10,11].

4.2 Prolate Spharoidal Wave Functions

Considering the space of square-integrable (i.e., finite-energy) functions, the PSWF's are special functions that can be constructed either in time- or frequency-domain [12]. We adopt a frequency-domain construction, well in line with our optimization formulation. The PSWF's denoted by $\{\Phi_n(f)\}$, with associated eigenvalues $\{\lambda_n\}$, are constructed with finite time support (limited for symmetry to $[-T_c/2, T_c/2]$) and specific bandwidth confinement to a range $[-B,B]$. These functions satisfy $\int_{-B}^{B}\Phi_n(u)\text{sinc}(f-u)du = T_c\lambda_n\Phi_n(f)$ and have the following two properties: i) they form a complete, orthonormal set over the space of finite-energy, time-limited pulses over $[-T_c/2, T_c/2]$, and ii) they form a complete, orthogonal set over the space of finite-energy functions over the interval $[-B,B]$:

$$(i)\ \int\limits_{-\infty}^{\infty}\Phi_n(f)\Phi_m(f)\,df = \delta_{nm}$$

$$(ii)\ \int\limits_{-B}^{B}\Phi_n(f)\Phi_m(f)df = \lambda_n\delta_{nm}$$

(18)

where $\delta_{mn} = 1$ for $m = n$ and 0 otherwise, and λ_n is the eigenvalue associated with the function $\Phi_n(f)$, and represents the fraction of energy of $\Phi_n(f)$ falling in the band $[-B,B]$. An important feature of PSWF's is that, among all time-limited functions with given duration T_c, they achieve, in decreasing order, the highest energy concentration in the band $[-B,B]$. This energy confinement is represented by the monotonically decaying

eigenvalues, which become essentially negligible when the order n exceeds the time-bandwidth product $2BT_c$ [12].

4.3 Problem Simplification

The PSWF properties lead to a significant reduction of the complexity of our optimization problem. Indeed, since the $\{\Phi_n(f)\}$ form a complete set for the space of functions $H(f)$ of interest, the following linear expansion is obtained:

$$H(f) = \sum_{n=0}^{\infty} x_n \Phi_n(f) \qquad (19)$$

where x_n is given by the inner product

$$<H, \Phi_n> = \int_{-\infty}^{\infty} H(f)\Phi_n(f)df \qquad (20)$$

Because the eigenvalues $\{\lambda_n\}$ decay rapidly to zero, a truncated series with a limited number N of PSWF's may be used. In addition, assuming even symmetry for the chip pulses of interest, we only need to keep the even-indexed $\Phi_n(f)$ (since the even-indexed functions are even and the odd-indexed ones are odd, as shown in [12]). The truncated series becomes:

$$H(f) \cong \sum_{n=0}^{N} x_{2n} \Phi_{2n}(f) \qquad (21)$$

Therefore, without significant loss of accuracy, we can reduce the problem formulated in (15)-(17) to a finite-dimensional low-complexity one, in terms of the expansion coefficients $\{x_{2n}\}$. This is compactly expressed by the following equations:

Minimize

$$F = \frac{\sum_{n=0}^{N} \dots \sum_{m=0}^{N} \gamma_1(n,\dots,m) \prod_{n=0}^{N} x_{2n}}{\left[\sum_{n=0}^{N} \sum_{m=0}^{N} \gamma_2(n,m) x_{2n} x_{2m}\right]\left[\sum_{n=0}^{N} \sum_{m=0}^{N} \gamma_3(n,m) x_{2n} x_{2m}\right]}$$

subject to $\begin{cases} \sum_{n=0}^{N} x_{2n}^2 = 1 \\ \sum_{n=0}^{N} \lambda_{2n} x_{2n}^2 = 1-\eta \end{cases}$

$$(22)$$

where the coefficients of the cost function can be checked to satisfy:

$$\gamma_1(n,\dots,m) = (4;0,1,\dots N) \int_{-\infty}^{\infty} \prod_{n=0}^{N} \Phi_{2n}(f)\,df$$

$$\gamma_2(n,m) = \int_{-\infty}^{\infty} \Phi_{2n}(f)\Phi_{2m}(f)\cos(\pi f)\,df \qquad (23)$$

$$\gamma_3(n,m) = \int_{-\infty}^{\infty} 2\pi f\, \Phi_{2n}(f)\Phi_{2m}(f)\sin(\pi f)\,df$$

with $(4;0,1,\dots,N)$ denoting the multinomial coefficient equal to $4!/(0!1!\dots N!)$.

Based on this approach, standard numerical optimization routines can be used to solve the problem formulation in (22). As will be shown in the next section, it is also found that for a practical range of bandwidth occupancies, it sufficient to use no more than four or five PSWF's in the expansion (21), which makes the numerical solution of the optimization problem computationally efficient.

5 Numerical Results

To illustrate the NC-DLL optimized pulse design methodology, we now present some novel chip waveforms and compare their performance to the conventional pulses discussed in Section 3. The design approach for obtaining these optimized chip pulses is based on maintaining a given bandwidth occupancy that is typically the same as the best performing conventional pulse and then solving the optimization problem (22) until a feasible solution that minimizes the cost function F is found. For the numerical results, two typical values for in-band power bandwidth measures are adopted, 99% and 99.9%, which correspond to out-of-band η factors of 1% and 0.1%, respectively. The bandwidth figures are taken in a range of $1/T_c$ to $3/T_c$ (which is quite typical in practice). It should also be noted that rectangular pulse shape has a particularly poor performance with respect to the 99% or 99.9% bandwidth (in excess of $10/T_c$) due to the slow decay in its power spectral density [10].

As shown in Table 3, with respect to the 99% bandwidth, the Half-Sine pulse is found to have the lowest occupancy of approximately $1.2/T_c$, so this value is used to design the OPT1 pulse as highlighted above. Similarly, for the 99.9% bandwidth, the Hamming pulse displays the lowest bandwidth of $1.6/T_c$ and this is used to design a second optimized pulse OPT2. An illustration of

these pulses is given in Figures 2 and 3. The expansion coefficients in terms of PSWF's are also given in Table 4.

The results of Table 3 show that the optimized pulses OPT1 and OPT2 achieve some small reduction (on the order of 10-15%) in the normalized tracking error factor M_c/κ. This indicates that, with Non-coherent DLL tracking, the half-sine pulse is quasi-optimal when taking into consideration the 99% bandwidth occupancy. On the other hand, the Hamming pulse is closest to optimal with respect to the 99.9% measure. Similar conclusions were also reported in [10] for coherent DLL tracking schemes. These observations are further confirmed by the results illustrated in Figs. 4 & 5 which show the optimal performance limit (in terms of minimum achievable cost factor $F = M_c/\kappa$) as a function of increasing 99% and 99.9% bandwidth occupancies, ranging from $1/T_c$ to $2/T_c$, and it can be seen that the proximity of the Half-sine and Hamming pulses to the lower bounds demonstrates the quasi-optimality of these pulses.

6   Conclusion

The paper addressed the code tracking performance of several chip waveforms in direct-sequence CDMA signalling using non-coherent delay-locked loops. Based on the linear NC-DLL model, it was shown that the tracking error variance is a function of the DLL S-curve slope at the origin and on the multiple-access interference power, both of which have a strong dependency on the chip waveform pulse shape. Some comparative results were then given to illustrate the tracking performance of several conventional chip waveforms, showing that non-rectangular pulses outperform the rectangular one, as was observed in previous work as well.

These observations motivated the work presented in the second part of the paper, where the problem of designing pulse shapes that minimize the residual tracking error was thoroughly addressed. An optimization approach with energy and bandwidth constraints, was presented in frequency-domain using an expansion of the chip waveform in terms of Prolate Spheroidal Wave Functions, which lead to a reduced complexity discrete optimization problem. Examples of optimized pulses were presented, and the results provided theoretical limits on the minimum achievable tracking jitter, showing that the Half-Sine pulse is quasi-optimum when considering 99% bandwidth, while the

Hamming pulse is closest to optimum when considering the 99.9% bandwidth measure.

Acknowledgment

References

[1] M.K. Simon, J.K. Omura, R.A Scholtz and B.K. Levitt, *Spread Spectrum Communications Handbook*, Rev. Ed., McGraw-Hill, 1994..

[2] A.J. Viterbi, *CDMA: Principles of Spread Spectrum Communication*, Addison-Wesley, 1995.

[3] R. Anjaria and R. Wyrwas, "The Effect of chip waveforms on CDMA systems in multipath fading noisy channels," *Proc. IEEE VTS*, pp. 672-675, May 1992.

[4] P.I. Dallas and F.N. Pavlidou, "Innovative chip waveforms in microcellular DS/CDMA packet mobile radio," *IEEE Trans. Comm.*, Vol.44, No.11, pp.1413-1416, Nov. 1996.

[5] Y. Huang and T-S. Ng, "A DS-CDMA system using dispreading sequences weighted by adjustable chip waveforms," *IEEE Trans. Comm.*, Vol.47, pp. 1884-1896, Dec. 1999.

[6] M. El-Tarhuni and M. Landolsi, "The effect of chip waveform shaping on the synchronization performance of DS-CDMA signals," *Proc. IEEE VTC*, Vol. 3, pp. 2427-2431, May 1999.

[7] S. Thayaparan, T.-S. Ng, and J. Wang, "Half-sine and triangular despreading chip waveforms for coherent delay-locked tracking in DS/SS systems," *IEEE Tran Comm*, vol. 48, pp. 1384-1391, 2000.

[8] C. Lee *et al*, "Analysis of detection performance of an energy detector for several chip waveforms in DS/SS communication," *IEEE MILCOM*, Vol. 1, pp. 123-127, 2001,

[9] X. Wu, C. Ling, and H. Xiang, "Despreading chip waveform design for coherent delay-locked tracking in DS/SS systems," *Proc. IEEE ICC*, Vol.1, pp. 631-635, May 2002.

[10] M. A. Landolsi, "Minimisation of timing jitter in CDMA code tracking," *IEE Electronics Letters*, vol. 40, pp. 1352-1353, 2004.

[11] M.A. Landolsi, "Performance Limits in DS-CDMA Timing Acquisition," *IEEE Trans. on Wireless Comm.* Vol. 6, No. 9, pp. 3248-3255, Sept. 2007

[12] D. Splepian and H. Pollak, "Prolate spheroidal wave functions, Fourier analysis and uncertainty", *Bell Sys. Tech. Jour.*, Vol. 40, No. 1, pp. 43-64, January 1961.
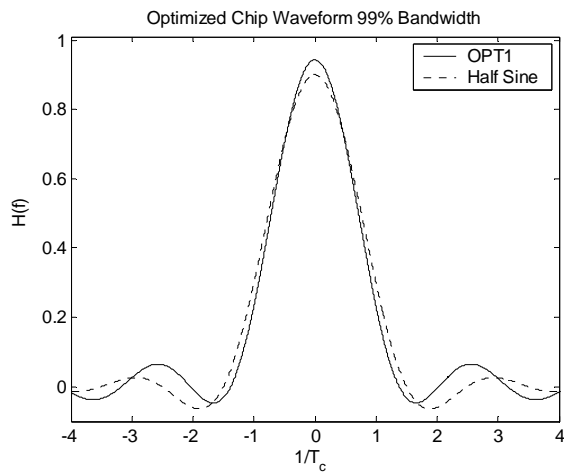
Fig. 2: Illustration of Optimized Chip Pulse OPT1
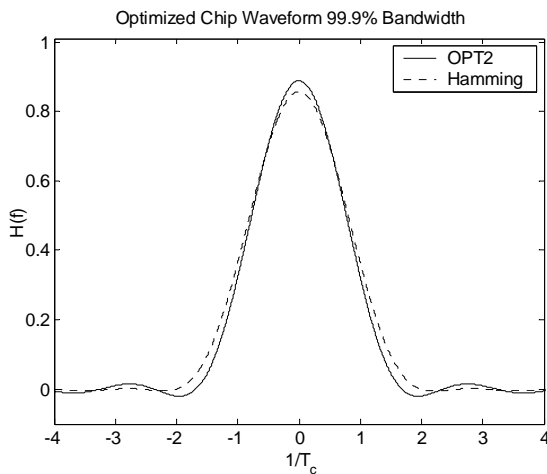
Fig. 3: Illustration of optimized chip pulse OPT2
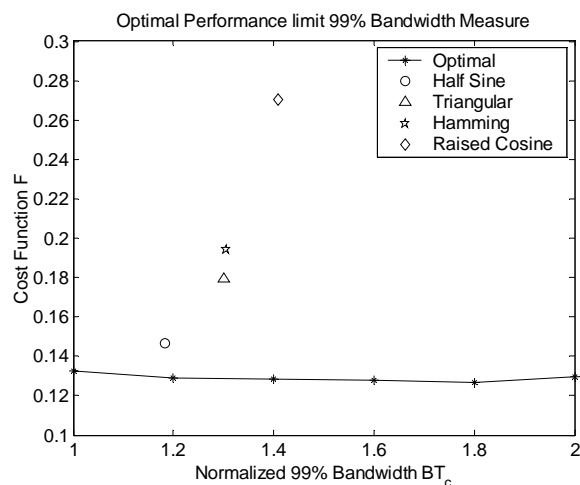
Fig. 4: Relative performance w.r.t minimum achievable limit (for 99% bandwidth measure)
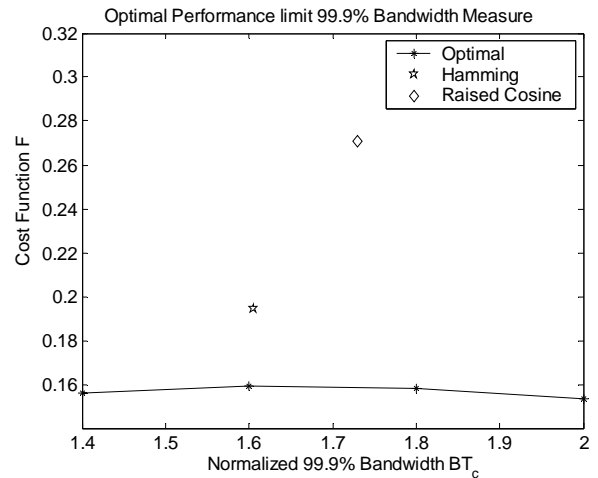
Fig. 5: Relative performance w.r.t minimum achievable limit (for 99.9% bandwidth measure)

PULSE	99% BT_c	99.9% BT_c	M_c / κ
Half-Sine	1.2	2.7	0.147
Triangular	1.3	3.1	0.180
Raised-Cosine	1.4	1.7	0.271
Hamming	1.3	1.6	0.194
OPT1	1.2	4.7	0.131
OPT2	1.2	1.6	0.160

Table 3: Comparative tracking performance of optimized chip pulses.

PULSE	x_0	x_2	x_4	x_6
OPT1	0.997E0	-0.654E-1	0.192E-1	0.323E-1
OPT2	0.999E0	-0.445E-1	0.663E-3	0.873E-4

Table 4: PSWF expansion coefficients of the optimized waveform pulses OPT1 and OPT2.